文章编号:1000-0887(2003)04-0357-10

复合材料层合剪切圆柱曲板在侧压作用下的后屈曲*

沈惠申

(上海交通大学 建筑工程与力学学院,上海 200030)

(我刊编委沈惠申来稿)

摘要: 基于 Reddy 高阶剪切变形理论的 Kármán-Donnell 型非线性壳体方程,给出复合材料层合剪切圆柱曲板在侧压作用下的后屈曲分析. 将壳体屈曲的边界层理论推广到复合材料层合剪切圆柱曲板受侧压作用的情况. 相应的奇异摄动法,用于确定圆柱曲板的屈曲荷载和后屈曲平衡路径. 分析中同时考虑非线性前屈曲变形和初始几何缺陷的影响. 数值算例给出完善和非完善,中等厚度正交铺设层合圆柱曲板的后屈曲荷载-挠度曲线. 讨论了横向剪切变形,曲板几何参数,铺层数,铺层方式和初始几何缺陷等各种参数变化的影响.

关 键 词: 结构稳定性; 屈曲; 后屈曲; 圆柱曲板; 高阶剪切变形理论; 壳体屈曲的边界层理论; 奇异摄动法

中图分类号: O343 **文献标识码:** A

引 言

纤维增强复合材料圆柱曲板已广泛用于航空,造船,汽车及其它工业部门. 对于圆柱曲板在轴压或扭矩作用下的屈曲和后屈曲已有过诸多研究. 相反,对于圆柱曲板在侧压作用下的屈曲问题则少有讨论,其中包括 Singer 等[1]的小挠度屈曲分析,Yamada 和 Croll[2]的非线性屈曲分析,Yamada[3]采用刚度降阶算法的弹塑性屈曲分析,Redekop 和 Makhoul[4]采用微分求积法的数值分析. 所有这些研究都是针对各向同性圆柱曲板,并基于经典壳体理论. 由于横向剪切弹性模量比面内弹性模量低得多,因而复合材料层合结构中横向剪切变形的影响要比各向同性材料结构中大得多. 再者,铺层方式对中厚曲板要比对薄曲板有更大的影响. 因此,在中等厚度复合材料层合圆柱曲板的分析中需要采用剪切变形理论. 最近,Shen[5~7]给出复合材料层合剪切圆柱壳在轴压、外压及其联合作用下的完整的后屈曲分析. 然而,至今尚无公开发表的文献讨论过复合材料层合剪切圆柱曲板在侧压作用下的后屈曲行为.

本文基于 Reddy 高阶剪切变形理论的 Kármán-Donnell 型非线性壳体方程,将沈惠申和陈铁云[8]提出的壳体屈曲的边界层理论推广到复合材料层合剪切圆柱曲板受侧压作用的情况. 相

* **收稿日期:** 2001-10-22; **修订日期:** 2003-01-10
基金项目: 国家自然科学基金资助项目(59975058)
作者简介: 沈惠申(1947—),男,浙江嘉善人,教授,博士,博士生导师(E-mail:hsshen@mail.sjtu.edu.cn).

应的奇异摄动法用于确定圆柱曲板的屈曲荷载和后屈曲平衡路径．分析中同时考虑非线性前屈曲变形和初始几何缺陷的影响，初始几何缺陷的形式取作和曲板初始屈曲模态一致．

1 基本方程

考虑复合材料层合圆柱曲板受侧向均布压力 q 作用．假定 $\bar{U}$、$\bar{V}$ 和 $\bar{W}$ 为对应右手坐标系 (X, Y, Z) 的位移分量，其中 X、Y 和 Z 分别为曲板中面轴向、周向和法向(向内指向为正)坐标．$\bar{\Psi}_x$ 和 $\bar{\Psi}_y$ 分别为中面法线相对 Y 和 X 轴的转角．坐标原点取在曲板中面角点．R 为曲率半径，t 为曲板厚度，a 为曲板长度，b 为曲板弧线宽度，如图1所示．以 $\bar{W}^*(X,Y)$ 和 $\bar{W}(X,Y)$ 分别表示曲板的初始几何缺陷和附加挠度，以 $\bar{F}(X,Y)$ 表示应力函数，即使 $\bar{N}_x = \bar{F}_{,yy}$，$\bar{N}_y = \bar{F}_{,xx}$ 和 $\bar{N}_{xy} = -\bar{F}_{,xy}$，其中逗号表示对相应坐标求导．

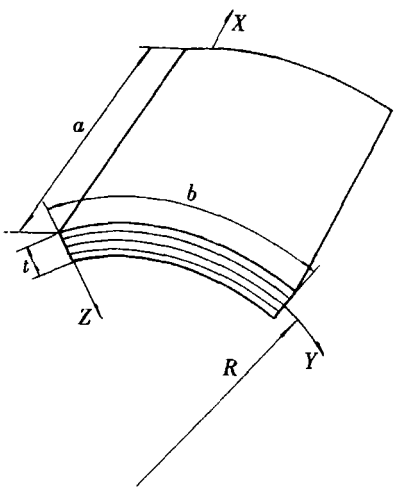

图1 层合圆柱曲板几何尺寸和坐标系

本文集中讨论中等厚度正交铺设层合圆柱曲板，中等厚度各向同性或单层正交各向异性圆柱曲板可作为特例处理．

Reddy 和 Liu[9] 曾发展一种简单的高阶剪切变形壳体理论，其中假定横向剪切变形沿壳体厚度方向呈抛物线型变化，而独立未知数和一阶剪切变形理论相同．基于 Reddy 高阶剪切变形理论，采用 Kármán 位移-应变关系，我们可以导得以法向挠度 $\bar{W}$(含初始几何缺陷 $\bar{W}^*$)，转角 $\bar{\Psi}_x$ 和 $\bar{\Psi}_y$，和应力函数 $\bar{F}$ 表示的广义 Kármán-Donnell 型非线性壳体方程

$$\tilde{L}_{11}(\bar{W}) - \tilde{L}_{12}(\bar{\Psi}_x) - \tilde{L}_{13}(\bar{\Psi}_y) + \tilde{L}_{14}(\bar{F}) - \frac{1}{R}\bar{F}_{,xx} = \tilde{L}(\bar{W} + \bar{W}^*, \bar{F}) + q, \tag{1}$$

$$\tilde{L}_{21}(\bar{F}) + \tilde{L}_{22}(\bar{\Psi}_x) + \tilde{L}_{23}(\bar{\Psi}_y) - \tilde{L}_{24}(\bar{W}) + \frac{1}{R}\bar{W}_{,xx} = -\frac{1}{2}\tilde{L}(\bar{W} + 2\bar{W}^*, \bar{W}), \tag{2}$$

$$\tilde{L}_{31}(\bar{W}) + \tilde{L}_{32}(\bar{\Psi}_x) - \tilde{L}_{33}(\bar{\Psi}_y) + \tilde{L}_{34}(\bar{F}) = 0, \tag{3}$$

$$\tilde{L}_{41}(\bar{W}) - \tilde{L}_{42}(\bar{\Psi}_x) + \tilde{L}_{43}(\bar{\Psi}_y) + \tilde{L}_{44}(\bar{F}) = 0, \tag{4}$$

其中线性算子 $\tilde{L}_{ij}(\ )$ 和非线性算子 $\tilde{L}(\ )$ 如文献[7]所定义．

边界支承假定为四边简支的，且无面内位移．那么，边界条件为

$$X = 0, a: \quad \bar{W} = \bar{U} = 0, \ \bar{\Psi}_y = 0, \ \bar{M}_x = \bar{P}_x = 0; \tag{5a~c}$$

$$Y = 0, b: \quad \bar{W} = \bar{V} = 0, \ \bar{\Psi}_x = 0, \ \bar{N}_{xy} = 0; \tag{5d~f}$$

其中 $\bar{M}_x$ 为单位长度弯矩，$\bar{P}_x$ 为高阶弯矩，如文献[9]所定义．面内不可移条件 $\bar{U} = 0$(沿 $X = 0, a$ 边界)和 $\bar{V} = 0$(沿 $Y = 0, b$ 边界)可用其均值代替，即

$$\int_0^b \int_0^a \frac{\partial \bar{U}}{\partial X} \mathrm{d}X \mathrm{d}Y = 0 \tag{6a}$$

或

$$\int_0^b \int_0^a \left[A_{11}^* \frac{\partial^2 \bar{F}}{\partial Y^2} + A_{12}^* \frac{\partial^2 \bar{F}}{\partial X^2} + \left(B_{11}^* - \frac{4}{3t^2} E_{11}^* \right) \frac{\partial \bar{\Psi}_x}{\partial X} + \left(B_{12}^* - \frac{4}{3t^2} E_{12}^* \right) \frac{\partial \bar{\Psi}_y}{\partial Y} - \right.$$

$$\frac{4}{3t^2}\left(E_{11}^*\frac{\partial^2\bar{W}}{\partial X^2}+E_{12}^*\frac{\partial^2\bar{W}}{\partial Y^2}\right)-\frac{1}{2}\left(\frac{\partial\bar{W}}{\partial X}\right)^2-\frac{\partial\bar{W}}{\partial X}\frac{\partial\bar{W}^*}{\partial X}\Big]\mathrm{d}X\mathrm{d}Y=0 \tag{6b}$$

和

$$\int_0^a\int_0^b\frac{\partial\bar{V}}{\partial Y}\mathrm{d}Y\mathrm{d}X=0 \tag{7a}$$

或

$$\int_0^a\int_0^b\Big[A_{22}^*\frac{\partial^2\bar{F}}{\partial X^2}+A_{12}^*\frac{\partial^2\bar{F}}{\partial Y^2}+\left(B_{21}^*-\frac{4}{3t^2}E_{21}^*\right)\frac{\partial\bar{\Psi}_x}{\partial X}+\left(B_{22}^*-\frac{4}{3t^2}E_{22}^*\right)\frac{\partial\bar{\Psi}_y}{\partial Y}-$$
$$\frac{4}{3t^2}\left(E_{21}^*\frac{\partial^2\bar{W}}{\partial X^2}+E_{22}^*\frac{\partial^2\bar{W}}{\partial Y^2}\right)+\frac{\bar{W}}{R}-\frac{1}{2}\left(\frac{\partial\bar{W}}{\partial Y}\right)^2-\frac{\partial\bar{W}}{\partial Y}\frac{\partial\bar{W}^*}{\partial Y}\Big]\mathrm{d}Y\mathrm{d}X=0. \tag{7b}$$

在式(6)和(7)及下式(9)中，$[A_{ij}^*]$、$[B_{ij}^*]$、$[D_{ij}^*]$、$[E_{ij}^*]$、$[F_{ij}^*]$ 和 $[H_{ij}^*](i,j=1,2,6)$ 为“约化”刚度矩阵，定义为

$$\begin{cases}\boldsymbol{A}^*=\boldsymbol{A}^{-1},\ \boldsymbol{B}^*=-\boldsymbol{A}^{-1}\boldsymbol{B},\ \boldsymbol{D}^*=\boldsymbol{D}-\boldsymbol{B}\boldsymbol{A}^{-1}\boldsymbol{B},\ \boldsymbol{E}^*=-\boldsymbol{A}^{-1}\boldsymbol{E},\\ \boldsymbol{F}^*=\boldsymbol{F}-\boldsymbol{E}\boldsymbol{A}^{-1}\boldsymbol{B},\ \boldsymbol{H}^*=\boldsymbol{H}-\boldsymbol{E}\boldsymbol{A}^{-1}\boldsymbol{E},\end{cases} \tag{8}$$

其中 A_{ij}、B_{ij} 等为曲板刚度系数，如文献[7]所定义.

2 分析方法与渐近解

这一节我们结合边界条件(5)来求解方程(1)至(4). 首先引进无量纲参数(以及下式(14)，(16)和(17)中 γ_{ijk} 如文献[7]所定义)

$$\begin{cases}x=\pi X/a,\ y=\pi Y/b,\ \beta=a/b,\ \bar{Z}=a^2/Rt,\\ \epsilon=(\pi^2R/a^2)[D_{11}^*D_{22}^*A_{11}^*A_{22}^*]^{1/4},\\ (W,W^*)=\epsilon(\bar{W},\bar{W}^*)/[D_{11}^*D_{22}^*A_{11}^*A_{22}^*]^{1/4},\ F=\epsilon^2\bar{F}/[D_{11}^*D_{22}^*]^{1/2},\\ (\Psi_x,\Psi_y)=\epsilon^2(\bar{\Psi}_x,\bar{\Psi}_y)(a/\pi)/[D_{11}^*D_{22}^*A_{11}^*A_{22}^*]^{1/4},\\ \gamma_{14}=[D_{22}^*/D_{11}^*]^{1/2},\ \gamma_{24}=[A_{11}^*/A_{22}^*]^{1/2},\gamma_5=-A_{12}^*/A_{22}^*,\\ (\gamma_{31},\gamma_{41})=(a^2/\pi^2)(A_{55}-8D_{55}/t^2+16F_{55}/t^4,A_{44}-\\ \qquad 8D_{44}/t^2+16F_{44}/t^4)/D_{11}^*,\\ (M_x,P_x)=\epsilon^2(\bar{M}_x,4\bar{P}_x/3t^2)a^2/\pi^2D_{11}^*[D_{11}^*D_{22}^*A_{11}^*A_{22}^*]^{1/4},\\ \gamma_q=q(3)^{3/4}aR^{3/2}[A_{11}^*A_{22}^*]^{1/8}/4\pi[D_{11}^*D_{22}^*]^{3/8},\ \lambda_q^*=(q/E_{22})\times10^3.\end{cases} \tag{9}$$

那么非线性方程(1)至(4)可表为如下无量纲形式

$$\epsilon^2L_{11}(W)-\epsilon L_{12}(\Psi_x)-\epsilon L_{13}(\Psi_y)+\epsilon\gamma_{14}L_{14}(F)-\gamma_{14}F_{,xx}=$$
$$\gamma_{14}\beta^2L(W+W^*,F)+\gamma_{14}\frac{4}{3}(3)^{1/4}\lambda_q\epsilon^{3/2}, \tag{10}$$
$$L_{21}(F)+\gamma_{24}L_{22}(\Psi_x)+\gamma_{24}L_{23}(\Psi_y)-\epsilon\gamma_{24}L_{24}(W)+\gamma_{24}W_{,xx}=$$
$$-\frac{1}{2}\gamma_{24}\beta^2L(W+2W^*,W), \tag{11}$$
$$\epsilon L_{31}(W)+L_{32}(\Psi_x)-L_{33}(\Psi_y)+\gamma_{14}L_{34}(F)=0, \tag{12}$$
$$\epsilon L_{41}(W)-L_{42}(\Psi_x)+L_{43}(\Psi_y)+\gamma_{14}L_{44}(F)=0, \tag{13}$$

其中

$$L_{11}(\quad)=\gamma_{110}\frac{\partial^4}{\partial x^4}+2\gamma_{112}\beta^2\frac{\partial^4}{\partial x^2\partial y^2}+\gamma_{114}\beta^4\frac{\partial^4}{\partial y^4},$$

$$L_{12}(\quad)=\gamma_{120}\frac{\partial^3}{\partial x^3}+\gamma_{122}\beta^2\frac{\partial^3}{\partial x\partial y^2},$$

$$L_{13}(\quad)=\gamma_{131}\beta\frac{\partial^3}{\partial x^2\partial y}+\gamma_{133}\beta^3\frac{\partial^3}{\partial y^3},$$

$$L_{14}(\quad)=\gamma_{140}\frac{\partial^4}{\partial x^4}+2\gamma_{142}\beta^2\frac{\partial^4}{\partial x^2\partial y^2}+\gamma_{144}\beta^4\frac{\partial^4}{\partial y^4},$$

$$L_{21}(\quad)=\frac{\partial^4}{\partial x^4}+2\gamma_{212}\beta^2\frac{\partial^4}{\partial x^2\partial y^2}+\gamma_{214}\beta^4\frac{\partial^4}{\partial y^4},$$

$$L_{22}(\quad)=\gamma_{220}\frac{\partial^3}{\partial x^3}+\gamma_{222}\beta^2\frac{\partial^3}{\partial x\partial y^2},$$

$$L_{23}(\quad)=\gamma_{231}\beta\frac{\partial^3}{\partial x^2\partial y}+\gamma_{233}\beta^3\frac{\partial^3}{\partial y^3},$$

$$L_{24}(\quad)=\gamma_{240}\frac{\partial^4}{\partial x^4}+2\gamma_{242}\beta^2\frac{\partial^4}{\partial x^2\partial y^2}+\gamma_{244}\beta^4\frac{\partial^4}{\partial y^4},$$

$$L_{31}(\quad)=\gamma_{31}\frac{\partial}{\partial x}+\gamma_{310}\frac{\partial^3}{\partial x^3}+\gamma_{312}\beta^2\frac{\partial^3}{\partial x\partial y^2},$$

$$L_{32}(\quad)=\gamma_{31}-\gamma_{320}\frac{\partial^2}{\partial x^2}-\gamma_{322}\beta^2\frac{\partial^2}{\partial y^2},$$

$$L_{33}(\quad)=\gamma_{331}\beta\frac{\partial^2}{\partial x\partial y},$$

$$L_{34}(\quad)=L_{22}(\quad),$$

$$L_{41}(\quad)=\gamma_{41}\beta\frac{\partial}{\partial y}+\gamma_{411}\beta\frac{\partial^3}{\partial x^2\partial y}+\gamma_{413}\beta^3\frac{\partial^3}{\partial y^3},$$

$$L_{42}(\quad)=L_{33}(\quad),$$

$$L_{43}(\quad)=\gamma_{41}-\gamma_{430}\frac{\partial^2}{\partial x^2}-\gamma_{432}\beta^2\frac{\partial^2}{\partial y^2},$$

$$L_{44}(\quad)=L_{23}(\quad),$$

$$L(\quad)=\frac{\partial^2}{\partial x^2}\frac{\partial^2}{\partial y^2}-2\frac{\partial^2}{\partial x\partial y}\frac{\partial^2}{\partial x\partial y}+\frac{\partial^2}{\partial y^2}\frac{\partial^2}{\partial x^2}.$$

(14)

对于大多数复合材料 $[D_{11}^*D_{22}^*A_{11}^*A_{22}^*]^{1/4}=(0.2-0.3)t$，由式(9)，当 $\bar{Z}=(a^2/Rt)>2.96$ 时，我们有 $\varepsilon<1$. 特别是对于各向同性圆柱曲板，我们有 $\varepsilon=\pi^2/\bar{Z}_V\beta^2[12(1-\nu^2)]^{1/2}$，其中 $\bar{Z}_V(=b^2/Rt)$ 在经典的线性屈曲分析中其值应大于 11.95(参见 Vol'mir[10])，在此种情况下，$\varepsilon<1$ 的条件总能满足，除非 $\beta<0.5$. 当 $\varepsilon<1$ 时，方程(10)至(13)即为边界层型方程. 利用此方程可同时考虑曲板非线性前屈曲变形、后屈曲大挠度和初始几何缺陷的影响.

边界条件(5)化为

$$x=0,\pi:\quad W=U=0,\ \Psi_y=0,\ M_x=P_x=0;\qquad(15a\sim c)$$

$$y=0,\pi:\quad W=V=0,\ \Psi_x=0,\ F_{,xy}=0.\qquad(15d\sim f)$$

由式(6)和(7)表征的面内边界条件化为

$$\int_0^\pi\int_0^\pi\Big[\Big(\gamma_{24}^2\beta^2\frac{\partial^2F}{\partial y^2}-\gamma_5\frac{\partial^2F}{\partial x^2}\Big)+\gamma_{24}\Big(\gamma_{511}\frac{\partial\Psi_x}{\partial x}+\gamma_{233}\beta\frac{\partial\Psi_y}{\partial y}\Big)-$$

$$\varepsilon\gamma_{24}\left(\gamma_{611}\frac{\partial^2 W}{\partial x^2}+\gamma_{244}\beta^2\frac{\partial^2 W}{\partial y^2}\right)-\frac{1}{2}\gamma_{24}\left(\frac{\partial W}{\partial x}\right)^2-\gamma_{24}\frac{\partial W}{\partial x}\frac{\partial W^*}{\partial x}\Big]\mathrm{d}x\mathrm{d}y=0 \tag{16}$$

和

$$\begin{aligned}\int_0^{\pi}\int_0^{\pi}\Big[&\left(\frac{\partial^2 F}{\partial x^2}-\gamma_5\beta^2\frac{\partial^2 F}{\partial y^2}\right)+\gamma_{24}\left(\gamma_{220}\frac{\partial \Psi_x}{\partial x}+\gamma_{522}\beta\frac{\partial \Psi_y}{\partial y}\right)-\\&\varepsilon\gamma_{24}\left(\gamma_{240}\frac{\partial^2 W}{\partial x^2}+\gamma_{622}\beta^2\frac{\partial^2 W}{\partial y^2}\right)+\gamma_{24}W-\\&\frac{1}{2}\gamma_{24}\beta^2\left(\frac{\partial W}{\partial y}\right)^2-\gamma_{24}\beta^2\frac{\partial W}{\partial y}\frac{\partial W^*}{\partial y}\Big]\mathrm{d}y=0.\end{aligned} \tag{17}$$

根据式(10)至(17),采用奇异摄动方法可确定完善和非完善,层合剪切圆柱曲板在侧压作用下的后屈曲行为. 假定方程(10)至(13)的解为

$$\begin{cases}W=w(x,y,\varepsilon)+\tilde{W}(x,\xi,y,\varepsilon)+\hat{W}(x,\zeta,y,\varepsilon),\\F=f(x,y,\varepsilon)+\tilde{F}(x,\xi,y,\varepsilon)+\hat{F}(x,\zeta,y,\varepsilon),\\\Psi_x=\psi_x(x,y,\varepsilon)+\tilde{\Psi}_x(x,\xi,y,\varepsilon)+\hat{\Psi}_x(x,\zeta,y,\varepsilon),\\\Psi_y=\psi_y(x,y,\varepsilon)+\tilde{\Psi}_y(x,\xi,y,\varepsilon)+\hat{\Psi}_y(x,\zeta,y,\varepsilon),\end{cases} \tag{18}$$

其中 ε 为摄动小参数(限于 $\bar{Z}>2.96$). $w(x,y,\varepsilon)$、$f(x,y,\varepsilon)$、$\psi_x(x,y,\varepsilon)$、$\psi_y(x,y,\varepsilon)$ 称为曲板的"外解"或正则解,$\tilde{W}(x,\xi,y,\varepsilon)$、$\tilde{F}(x,\xi,y,\varepsilon)$、$\tilde{\Psi}_x(x,\xi,y,\varepsilon)$、$\tilde{\Psi}_y(x,\xi,y,\varepsilon)$ 和 $\hat{W}(x,\zeta,y,\varepsilon)$、$\hat{F}(x,\zeta,y,\varepsilon)$、$\hat{\Psi}_x(x,\zeta,y,\varepsilon)$、$\hat{\Psi}_y(x,\zeta,y,\varepsilon)$ 分别为 $x=0$ 和 $x=\pi$ 端的边界层解,且边界层变量 ξ 和 ζ 定义为

$$\xi=x/\sqrt{\varepsilon},\quad \zeta=(\pi-x)/\sqrt{\varepsilon} \tag{19}$$

(这意味着对于各向同性圆柱曲板,边界层宽度为 $\sqrt{Rt}$ 量级). 将式(18)中的正则解和边界层解展为如下渐近展开式

$$\begin{cases}w(x,y,\varepsilon)=\sum_{j=1}\varepsilon^{j/2}w_{j/2}(x,y),\ f(x,y,\varepsilon)=\sum_{j=0}\varepsilon^{j/2}f_{j/2}(x,y),\\\psi_x(x,y,\varepsilon)=\sum_{j=1}\varepsilon^{j/2}(\psi_x)_{j/2}(x,y),\ \psi_y(x,y,\varepsilon)=\sum_{j=1}\varepsilon^{j/2}(\psi_y)_{j/2}(x,y);\end{cases} \tag{20a}$$

$$\begin{cases}\tilde{W}(x,\xi,y,\varepsilon)=\sum_{j=0}\varepsilon^{j/2+1}\tilde{W}_{j/2+1}(x,\xi,y),\\\tilde{F}(x,\xi,y,\varepsilon)=\sum_{j=0}\varepsilon^{j/2+2}\tilde{F}_{j/2+2}(x,\xi,y),\\\tilde{\Psi}_x(x,\xi,y,\varepsilon)=\sum_{j=0}\varepsilon^{(j+3)/2}(\tilde{\Psi}_x)_{(j+3)/2}(x,\xi,y),\\\tilde{\Psi}_y(x,\xi,y,\varepsilon)=\sum_{j=0}\varepsilon^{j/2+2}(\tilde{\Psi}_y)_{j/2+2}(x,\xi,y);\end{cases} \tag{20b}$$

$$\begin{cases}\hat{W}(x,\zeta,y,\varepsilon)=\sum_{j=0}\varepsilon^{j/2+1}\hat{W}_{j/2+1}(x,\zeta,y),\\\hat{F}(x,\zeta,y,\varepsilon)=\sum_{j=0}\varepsilon^{j/2+2}\hat{F}_{j/2+2}(x,\zeta,y),\\\hat{\Psi}_x(x,\zeta,y,\varepsilon)=\sum_{j=0}\varepsilon^{(j+3)/2}(\hat{\Psi}_x)_{(j+3)/2}(x,\zeta,y),\\\hat{\Psi}_y(x,\zeta,y,\varepsilon)=\sum_{j=0}\varepsilon^{j/2+2}(\hat{\Psi}_y)_{j/2+2}(x,\zeta,y).\end{cases} \tag{20c}$$

曲板初始屈曲模态假定为

$$w_2(x,y)=A_{11}^{(2)}\sin mx\sin ny. \tag{21}$$

曲板初始几何缺陷假定具有相同的形式，即

$$W^*(x,y,\varepsilon) = \varepsilon^2 a_{11}^* \sin mx \sin ny = \varepsilon^2 \mu A_{11}^{(2)} \sin mx \sin ny, \tag{22}$$

其中 $\mu = a_{11}^*/A_{11}^{(2)}$ 为缺陷参数.

将式(18)至(20)代入方程(10)至(13)，可得正则解和边界层解各自应满足的三组摄动方程，利用式(21)和(22)逐级求解这些摄动方程组，并在曲板 $x = 0$ 和 $x = \pi$ 两端匹配正则解和边界层解，可以导得大挠度渐近解

$$\begin{aligned} W = {} & \varepsilon^{3/2}\Big[A_{00}^{(3/2)} - A_{00}^{(3/2)}\Big(a_{01}^{(3/2)}\cos\phi\frac{x}{\sqrt{\varepsilon}} + a_{10}^{(3/2)}\sin\phi\frac{x}{\sqrt{\varepsilon}}\Big)\exp\Big(-\alpha\frac{x}{\sqrt{\varepsilon}}\Big) - \\ & A_{00}^{(3/2)}\Big(a_{01}^{(3/2)}\cos\phi\frac{\pi-x}{\sqrt{\varepsilon}} + a_{10}^{(3/2)}\sin\phi\frac{\pi-x}{\sqrt{\varepsilon}}\Big)\exp\Big(-\alpha\frac{\pi-x}{\sqrt{\varepsilon}}\Big) + \\ & \varepsilon^2[A_{11}^{(2)}\sin mx\sin ny] + \varepsilon^3[A_{11}^{(3)}\sin mx\sin ny] + \\ & \varepsilon^4[A_{00}^{(4)} + A_{20}^{(4)}\cos 2mx + A_{02}^{(4)}\cos 2ny] + O(\varepsilon^5), \end{aligned} \tag{23}$$

$$\begin{aligned} F = {} & -\frac{1}{2}B_{00}^{(0)}\Big(\beta^2x^2 + a_1\frac{y^2}{2}\Big) + \varepsilon\Big[-\frac{1}{2}B_{00}^{(1)}\Big(\beta^2x^2 + a_1\frac{y^2}{2}\Big)\Big] + \\ & \varepsilon^2\Big[-\frac{1}{2}B_{00}^{(2)}\Big(\beta^2x^2 + a_1\frac{y^2}{2}\Big) + B_{11}^{(2)}\sin mx\sin ny\Big] + \\ & \varepsilon^{5/2}\Big[A_{00}^{(3/2)}\Big(b_{01}^{(5/2)}\cos\phi\frac{x}{\sqrt{\varepsilon}} + b_{10}^{(5/2)}\sin\phi\frac{x}{\sqrt{\varepsilon}}\Big)\exp\Big(-\alpha\frac{x}{\sqrt{\varepsilon}}\Big) + \\ & A_{00}^{3/2}\Big(b_{01}^{(5/2)}\cos\phi\frac{\pi-x}{\sqrt{\varepsilon}} + b_{10}^{(5/2)}\sin\phi\frac{\pi-x}{\sqrt{\varepsilon}}\Big)\exp\Big(-\alpha\frac{\pi-x}{\sqrt{\varepsilon}}\Big)\Big] + \\ & \varepsilon^3\Big[-\frac{1}{2}B_{00}^{(3)}\Big(\beta^2x^2 + a_1\frac{y^2}{2}\Big)\Big] + \varepsilon^4\Big[-\frac{1}{2}B_{00}^{(4)}\Big(\beta^2x^2 + a_1\frac{y^2}{2}\Big) + \\ & B_{11}^{(4)}\sin mx\sin ny + B_{20}^{(4)}\cos 2mx + B_{02}^{(4)}\cos 2ny\Big] + O(\varepsilon^5), \end{aligned} \tag{24}$$

$$\begin{aligned} \Psi_x = {} & \varepsilon^2\Big[C_{11}^{(2)}\cos mx\sin ny + \Big(c_{01}^{(2)}\cos\phi\frac{x}{\sqrt{\varepsilon}} + c_{10}^{(2)}\sin\phi\frac{x}{\sqrt{\varepsilon}}\Big)\exp\Big(-\alpha\frac{x}{\sqrt{\varepsilon}}\Big) + \\ & \Big(c_{01}^{(2)}\cos\phi\frac{\pi-x}{\sqrt{\varepsilon}} + c_{10}^{(2)}\sin\phi\frac{\pi-x}{\sqrt{\varepsilon}}\Big)\exp\Big(-\alpha\frac{\pi-x}{\sqrt{\varepsilon}}\Big)\Big] + \\ & \varepsilon^3[C_{11}^{(3)}\cos mx\sin ny] + \varepsilon^4[C_{11}^{(4)}\cos mx\sin ny + C_{20}^{(4)}\sin 2mx] + O(\varepsilon^5), \end{aligned} \tag{25}$$

$$\begin{aligned} \Psi_y = {} & \varepsilon^2[D_{11}^{(2)}\sin mx\cos ny] + \varepsilon^3[D_{11}^{(3)}\sin mx\cos ny] + \\ & \varepsilon^4[D_{11}^{(4)}\sin mx\cos ny + D_{02}^{(4)}\sin 2ny] + O(\varepsilon^5). \end{aligned} \tag{26}$$

为了满足沿 $y = 0,\pi$ 直线边界 $w_{3/2} = 0$ 的条件，将式(23)中 $A_{00}^{(3/2)}$ 沿 y 向展成 Fourier 级数，即

$$\frac{4}{\pi}A_{00}^{(3/2)}\sum_{j=1,3,\cdots}\frac{1}{j}\sin jy, \tag{27}$$

而在 x 向仍保持为常数. 由式(23)可见，由于边界层解的贡献，曲板前屈曲变形是非线性的.

式(23)至(26)中各系数相互联系，皆可表为 $A_{11}^{(2)}$ 的函数，为简洁起见，具体表达式不再给出，但 a_1、α 和 ϕ 将在附录中给出.

进一步，将式(23)至(26)代入式(16)和(17)，我们可以导得后屈曲平衡路径

$$\lambda_q = \frac{1}{4}(3)^{3/4}\varepsilon^{-3/2}[\lambda_q^{(0)} + \lambda_q^{(2)}(A_{11}^{(2)}\varepsilon^2)^2 + \cdots]. \tag{28}$$

式(28)中，$(A_{11}^{(2)}\varepsilon^2)$ 可视为二次摄动参数，其值与曲板最大无量纲挠度有关，即

$$A_{11}^{(2)}\varepsilon^2 = W_m - \Theta_1 W_m^2 + \cdots, \tag{29a}$$

其中 W_m 为曲板最大无量纲挠度，假定取在 $(x,y) = (\pi/2m, \pi/2n)$ 点，且

$$W_m = \frac{1}{C_3}\left[\varepsilon \frac{t}{[D_{11}^* D_{22}^* A_{11}^* A_{22}^*]^{1/4}} \frac{\bar{W}}{t} + \Theta_2\right], \tag{29b}$$

式(28)和(29)中所有其它符号在附录中给出.

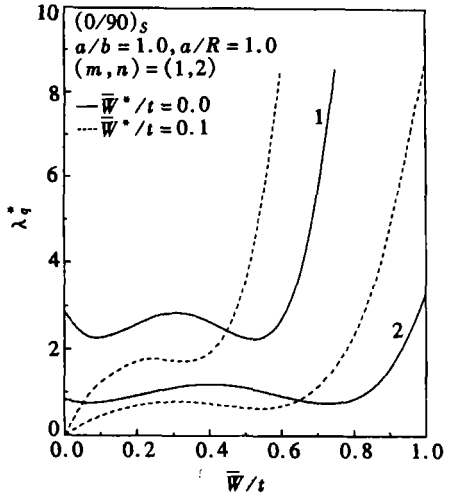

1: $b/t = 20$; 2: $b/t = 30$

图 2 宽厚比对 $(0/90)_S$ 层合圆柱曲板后屈曲行为的影响

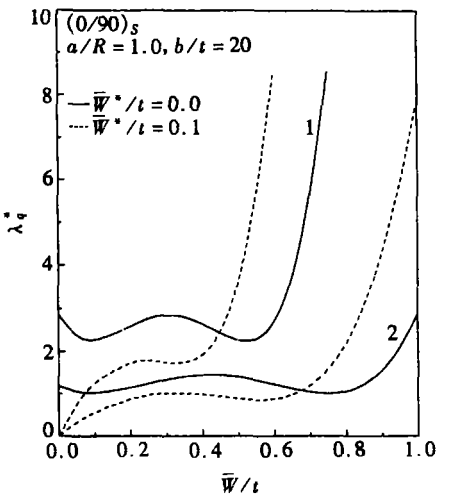

1: $a/b = 1.0$, $(m,n) = (1,2)$;
2: $a/b = 1.5$, $(m,n) = (1,1)$

图 3 长宽比对 $(0/90)_S$ 层合圆柱曲板后屈曲行为的影响

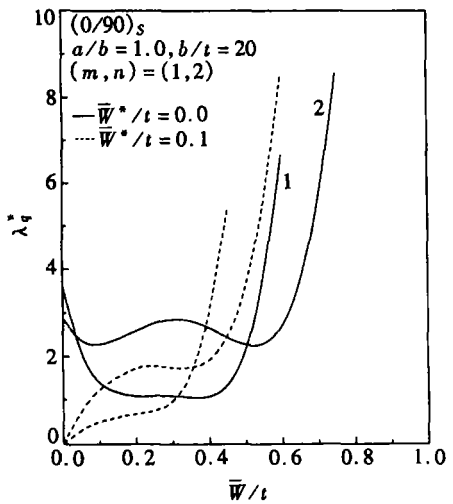

1: $a/R = 0.5$; 2: $a/R = 1.0$

图 4 长径比对 $(0/90)_S$ 层合圆柱曲板后屈曲行为的影响

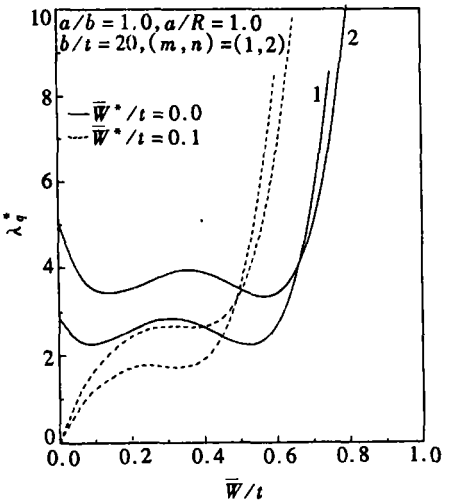

1: $(0/90)_S$; 2: $(0/90)_{4S}$

图 5 铺层数对对称正交铺设层合圆柱曲板后屈曲行为的影响

式(28)和(29)可用于复合材料层合剪切圆柱曲板在侧压作用下的后屈曲荷载-挠度曲线计算. 对于完善曲板取 $\bar{W}^*/t = 0$(或 $\mu = 0$)，并取 $\bar{W}/t = 0$(注意 $W_m \neq 0$)，我们容易求得屈曲荷载，其相应的屈曲模态为 (m,n)，分别对应 X 向和 Y 向的半波数.

3 数值算例和讨论

本节给出对称和反对称正交铺设层合圆柱曲板的数值结果，其中第一铺层对应曲板最外层．在所有算例中，每层层板厚度相等，材料性能常数取为：E_{11} = 130 GPa，E_{22} = 7 GPa，G_{12} = G_{13} = 6 GPa，G_{23} = 4.2 GPa 和 ν_{12} = 0.28．图 2 至图 6 为参数分析的主要结果，以无量纲形式给出．所有图中 $\bar{W}^*/t$ 和 $\bar{W}/t$ 分别表示曲板无量纲初始几何缺陷和附加的挠度．

图 2 给出完善（$\bar{W}^*/t$ = 0）和非完善（$\bar{W}^*/t$ = 0.1），$(0/90)_S$ 对称正交铺设层合圆柱曲板，对应不同宽厚比 b/t（= 20 和 30）时的后屈曲荷载 - 挠度曲线．图 3 则给出不同长宽比 a/b（= 1.0 和 1.5）对 $(0/90)_S$ 层合圆柱曲板后屈曲行为的影响．由图可见“跳跃”式的后屈曲平衡路径．这与完整壳体在外压作用下的后屈曲平衡路径完全不同（参见 Shen[7]）．同时可以看出，当 b/t 由 20 增加到 30，或 a/b 由 1.0 增加到 1.5，屈曲荷载降低，且当挠度较大时，后屈曲平衡路径变得相当低．

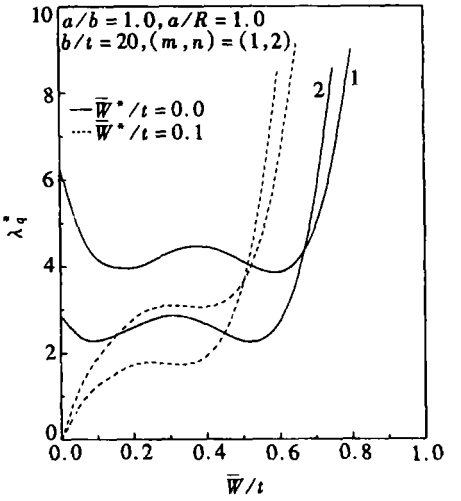

1:$(0/90)_{2T}$; 2:$(0/90)_S$

图 6 $(0/90)_{2T}$ 和 $(0/90)_S$ 正交铺设层合圆柱曲板后屈曲荷载-挠度曲线比较

图 4 给出不同长径比 a/R（= 0.5 和 1.0）对 $(0/90)_S$ 层合圆柱曲板后屈曲行为的影响．结果显示，a/R = 0.5 的曲板有较高的屈曲荷载，但在 $\bar{W}/t$ < 0.5 的范围内后屈曲强度较低．

图 5 给出不同铺层数 N（= 4 和 8）对对称正交铺设层合圆柱曲板后屈曲行为的影响．注意到曲板厚度 t 保持不变，因此，随着铺层数增加单层层板厚度减小．图示表明，屈曲荷载和后屈曲强度随着铺层数的增加而增加．

图 6 给出 $(0/90)_{2T}$ 和 $(0/90)_S$ 正交铺设层合圆柱曲板后屈曲荷载 - 挠度曲线比较．图示表明，二者相比，$(0/90)_{2T}$ 圆柱曲板有较高的屈曲荷载和后屈曲强度．

$(0/90)_{2T}$ 和 $(0/90)_S$ 正交铺设层合圆柱曲板在侧压作用下的屈曲荷载的部分计算结果列在表 1 中，以供比较．

表 1 正交铺设层合圆柱曲板屈曲荷载 $(q/E_{22})\times10^3$ 比较

（E_{11} = 130 GPa，E_{22} = 7 GPa，G_{12} = G_{13} = 6 GPa，G_{23} = 4.2 GPa 和 ν_{12} = 0.28）

a/b	a/R	b/t	$(0/90)_S$	$(0/90)_{2T}$
1.0	1.0	20	2.859 1(1,2)*	6.273 7(1,2)
1.0	1.0	30	0.840 7(1,2)	1.573 4(1,2)
1.0	0.5	20	3.582 1(1,2)	8.421 1(1,1)
1.5	1.0	20	1.183 3(1,1)	1.521 5(1,1)

* 括号里的值表示屈曲模态 (m,n)

4 结 语

基于 Reddy 高阶剪切变形理论的 Kármán-Donnell 型非线性壳体方程，给出复合材料层合

剪切圆柱曲板在侧压作用下完整的后屈曲分析．分析中同时考虑非线性前屈曲变形和初始几何缺陷的影响．壳体屈曲的边界层理论，被推广到复合材料层合剪切圆柱曲板，受侧压作用的情况．相应的奇异摄动法用于确定圆柱曲板的屈曲荷载和后屈曲平衡路径．数值算例给出完善和非完善，中等厚度正交铺设层合圆柱曲板的后屈曲荷载-挠度曲线．计算结果表明，侧压作用下圆柱曲板的后屈曲行为依赖于曲板本身的特性．和侧压作用下完整圆柱壳体不同，即便是完善圆柱曲板也有复杂的"跳跃"式后屈曲行为．计算结果同时表明，横向剪切变形、曲板几何参数、铺层数、铺层方式和初始几何缺陷对复合材料层合剪切圆柱曲板后屈曲行为有显著影响．

附　录

式(28)和(29)中

$$
\begin{cases}
\Theta_1 = \dfrac{1}{C_3\gamma_{24}}\left(1-\dfrac{1}{2}a_1\gamma_5\right)\lambda_q^{(2)},\ \Theta_2 = -\dfrac{1}{\gamma_{24}}\left(1-\dfrac{1}{2}a_1\gamma_5\right)\lambda_q^{(2)},\\
\lambda_q^{(0)} = \left\{\dfrac{\gamma_{24}m^4}{C_2(1+\mu)g_{06}} + \dfrac{\gamma_{24}m^2}{C_2(1+\mu)^2}\dfrac{g_{05}+(1+\mu)g_{07}}{g_{06}}\varepsilon + \right.\\
\qquad \dfrac{1}{\gamma_{14}C_2(1+\mu)}\left[g_{08}+\gamma_{14}\gamma_{24}\dfrac{g_{05}}{g_{06}}\dfrac{(1+\mu)g_{07}-\mu(2+\mu)g_{05}}{(1+\mu)^2}\right]\varepsilon^2 -\\
\qquad \dfrac{\mu}{(1+\mu)^2}\dfrac{g_{05}}{\gamma_{14}m^2C_2}\left[1+\dfrac{g_{05}}{(1+\mu)m^2}\varepsilon\right]\times\\
\qquad \left.\left[g_{08}+\gamma_{14}\gamma_{24}\dfrac{g_{05}}{g_{06}}\dfrac{(1+\mu)g_{07}+g_{05}}{(1+\mu)^2}(2+\mu)\right]\varepsilon^3\right\},\\
\lambda_q^{(2)} = \left\{\dfrac{m^4n^2\beta^2}{4g_{06}}\left[2\gamma_{24}(1+\mu)(2+\mu)+\dfrac{1}{4}\dfrac{\gamma_{24}g_{06}g_{13}}{n^2\beta^2C_2}(1+2\mu)-\right.\right.\\
\qquad \dfrac{\gamma_{24}n^2\beta^2g_{06}}{C_2(1+\mu)g_{06}-2a_1m^6g_{10}}\left(2(1+\mu)^2+\dfrac{1}{2}\dfrac{a_1m^2}{C_2}(1+2\mu)+\right.\\
\qquad \left.\left.\dfrac{(1+2\mu)g_{06}+8m^4g_{10}(1+\mu)}{g_{06}}(2+\mu)\right)\right]+\\
\qquad \left.\dfrac{\gamma_{24}}{8\gamma_5}\left[m^2\left(1+2\mu+\dfrac{1}{\pi\alpha}\varepsilon^{1/2}\right)-2g_{05}\varepsilon+\dfrac{g_{05}^2}{m^2}\varepsilon^2\right]\right\}.
\end{cases}
\tag{A.1}
$$

在上式中(其中 g_{ij} 和 g_{ijk} 如文献[7]所给出)

$$
\begin{cases}
a_1 = \dfrac{2\gamma_5}{\gamma_{24}^2},\ b_1 = \left[\dfrac{\gamma_{14}\gamma_{24}\gamma_{320}^2}{g_{16}}\right]^{1/2},\ c_1 = \gamma_{14}\gamma_{24}\gamma_{320}\dfrac{g_{15}}{2g_{16}},\\
C_2 = n^2\beta^2+\dfrac{1}{2}a_1m^2,\ C_3 = 1-\dfrac{g_{05}}{m^2}\varepsilon,\\
\alpha = [(b_1-c_1)/2]^{1/2},\ \phi = [(b_1+c_1)/2]^{1/2}.
\end{cases}
\tag{A.2}
$$

[参　考　文　献]

[1] Singer J, Meer A, Baruch M. Buckling of cylindrical panels under lateral pressure[J]. *Aeronautical Journal*, 1969, **73**(698): 169—172.

[2] Yamada S, Croll J G A. Buckling behavior of pressure loaded cylindrical panels[J]. *Journal of Engineering Mechanics ASCE*, 1989, **115**(2): 327—334.

[3] Yamada S. Buckling analysis for design of pressurized cylindrical shell panels[J]. *Engineering Structures*, 1997, **19**(5): 352—359.

[4] Redekop D, Makhoul E. Use of the differential quadrature method for the buckling analysis of cylindrical shell panels[J]. *Structural Engineering and Mechanics*, 2000, **10**(5): 451—462.

[5] SHEN Hui-shen. Postbuckling of shear deformable laminated cylindrical shells[J]. *Journal of Engineering Mechanics ASCE*, 2002, **128**(3): 296—307.

[6] SHEN Hui-shen. Li Q S. Thermomechanical postbuckling of shear deformable laminated cylindrical shells with local geometric imperfections[J]. *International Journal of Solids and Structures*, 2002, **39**(17): 4525—4542.

[7] SHEN Hui-shen. Postbuckling of shear deformable cross-ply laminated cylindrical shells under combined external pressure and axial compression[J]. *International Journal of Mechanical Sciences*, 2001, **43**(11): 2493—2523.

[8] 沈惠申,陈铁云.圆柱薄壳在外压作用下屈曲的边界层理论[J].应用数学和力学,1988,9(6):515—528.

[9] Reddy J N, Liu C F. A higher-order shear deformation theory of laminated elastic shells[J]. *International Journal of Engineering Science*, 1985, **23**(3): 319—330.

[10] Vol'mir A A. Flexible Plates and Shells[Z]. AFFDL-TR-66-216, 1967.

Postbuckling of Pressure-Loaded Shear Deformable Laminated Cylindrical Panels

SHEN Hui-shen

(*School of Civil Engineering and Mechanics, Shanghai Jiaotong University, Shanghai* 200030, *P. R. China*)

Abstract: A postbuckling analysis is presented for a shear deformable laminated cylindrical panel of finite length subjected to lateral pressure. The governing equations are based on Reddy's higher order shear deformation shell theory with von Kármán-Donnell-type of kinematic nonlinearity. The nonlinear prebuckling deformations and initial geometric imperfections of the panel are both taken into account. A boundary layer theory of shell buckling, which includes the effects of nonlinear prebuckling deformations, large deflections in the postbuckling range, and initial geometric imperfections of the shell, is extended to the case of shear deformable laminated cylindrical panels under lateral pressure. A singular perturbation technique is employed to determine the buckling loads and postbuckling equilibrium paths. The numerical illustrations concern the postbuckling response of perfect and imperfect, moderately thick, cross-ply laminated cylindrical panels. The effects played by transverse shear deformation, panel geometric parameters, total number of plies, fiber orientation, and initial geometric imperfections are studied.

Key words: structural stability; buckling; postbuckling; cylindrical panel; higher order shear deformable shell theory; boundary layer theory of shell buckling; singular perturbation technique